Supporting Information

The mitochondrial ribosomal protein L13 is critical for the structural and functional integrity of the mitochondrion in *Plasmodium falciparum*

Hangjun Ke[1*], Swati Dass[1], Joanne M. Morrisey[1], Michael W. Mather[1], and Akhil B. Vaidya[1]

[1]From the Center for Molecular Parasitology, Department of Microbiology and Immunology, Drexel University College of Medicine, Philadelphia, PA 19129, USA

Running title: Mitochondrial ribosomal protein L13 in *Plasmodium falciparum*

*To whom correspondence should be addressed: Hangjun Ke, Center for Molecular Parasitology, Department of Microbiology and Immunology, Drexel University College of Medicine, 2900 Queen Lane, Philadelphia, PA 19129, USA. Tel.: (215) 991-8448; Fax: (215) 848-2271; E-mail: hk84@drexel.edu

List of Content:

Materials and methods

1. Plasmid construction.

1) The genomic region of the putative *P. falciparum* mitochondrial ribosomal subunit L13 (PfmRPL13, PF3D7_0214200) is 900 bp, which includes one intron of 261 bp from +90 to +350. For localization studies, the coding region of PfmRPL13 was amplified from cDNA of wildtype 3D7 parasites using primers P1 and P2 (Table S1). The PfmRPL13 fragment was then cloned into the pLNmRL2 vector (1) via *Avr* II and *Bsi*W I restriction endonucleases to yield a copy of PfmRPL13 tagged with 3HA or GFP at the C-termini, namely pLN-PfmRPL13-3HA or pLN-PfmRPL13-GFP, respectively. The pLNmRL2 vectors with 3HA or GFP tags were derived from the original pLN-ENR-GFP plasmid generated by Nkrumah *et al.* (2).

2) The pL6 and pUF1-Cas9 vectors were kindly provided by Dr. Lopez-Rubio (3). The pL6 plasmid bears a cassette for expressing a single guide RNA (sgRNA), namely the *P. falciparum* U6 small nuclear RNA regulatory system (3). To perform knockout studies mediated with CRISPR/Cas9, two homologous regions of PfmRPL13, 5HR and 3HR, and a gRNA were cloned into the pL6 vector. The homologous regions were amplified from 3D7 genomic DNA using P3+P4 (5HR) and P5+P6 (3HR) primer pairs (Table S1) and were sequentially cloned into the pL6 vector, resulting in a primitive PfmRPL13 knockout construct without gRNA (pL6-PfmRPL13-pKO). The 5HR is a 608 bp fragment from -529 to +79 of the PfmRPL13 genomic region and was cloned via *Sac* II and *Afl* II. The 3HR is a 681 bp fragment from positions +388 to +1068 and was cloned via *Eco*R I and *Nco* I. To search for the best gRNA for CRISPR/Cas9 mediated knockout, a fragment between the two homologous regions (308 bp) was analyzed by the Eukaryotic Pathogen CRISPR guide RNA Design Tool (http://grna.ctegd.uga.edu/). From all potential hits, the best available gRNA was chosen based on its high efficiency score and zero off-target matches. This gRNA was named RL13KO_gRNA, and the sequence was 5'-GGCATATTCTTCTTTAAAAA(TGG)-3'. It was cloned into the pL6-PfmRPL13-pKO vector via InFusion cloning according to the manufacture's guidance (Clontech® Laboratories, Inc.). Briefly, the

pL6-PfmRPL13-pKO vector was linearized with *Btg*Z I. We synthesized a 60 bp oligo that harbors a 20 bp sequence homologous to the segment immediately upstream of the *Btg*Z I site of the pL6-PfmRPL13-pKO vector, a 20 bp RL13KO_gRNA sequence and another 20 bp sequence homologous to the segment immediately downstream of the *Btg*Z I site of the vector. The reverse complement strand (60 bp) was also synthesized. These two 60 bp oligoes, RL13-oligo1 (P7) and RL13-oligo2 (P8), were then mixed in a 1:1 mixture of Buffer 2 and Buffer 4 (New England Biolabs®, Inc.), heated at 95 ºC for 5 min and gradually cooled down to room temperature. The annealed oligoes and the linearized pL6-PfmRPL13-pKO vector were then joined by InFusion cloning to yield the pL6-PfmRPL13-KO vector for knockout studies. The N20 of RL13KO_gRNA (P9) and a vector primer from the pL6 vector (P10) were used to diagnose positive clones. Another oligo (P11), 71bp downstream of *Btg*Z I site, was used to sequence the cloned gRNA.

3) To do knockdown studies, we utilized the TetR-DOZI-aptamer system, recently developed and kindly provided by Dr. Jacquin Niles' group at MIT (4). Based on this system (4), Spillman and Beck *et al.* developed a double crossover integration strategy to insert aptamer copies mediated with the CRISPR/Cas9 system (5). They developed a pAll-In-One (pAIO) vector which contained Cas9 infused with the yDHODH gene (6) and elements for expressing a gRNA (5). Dr. Spillman and Dr. Beck kindly provided us with this all-in-one vector. We then cloned two gRNAs of PfmRPL13 into the pAIO vector via InFusion cloning as described above, generating pAIO-RL13-gRNA1 and pAIO-RL13-gRNA2, respectively. These two gRNAs of PfmRPL13 were located immediately upstream and downstream of the stop codon of PfmRPL13, respectively. The oligoes used for making these gRNA constructs and diagnostic PCRs were listed in Table S1 from P12 to P17.

The original pMG75-ATP4 vector (4) contains two attP sites for quick site specific genome insertions via the attBXattP system in attB positive strains (2). This facilitated a quick knockdown using the TetR-DOZI-aptamer system at an ectopical site, but not at the endogenous locus. An attP site is not required for

endogenous gene insertion. To remove two attP sites from the pMG75-ATP4 vector, pMG75-ATP4 was digested with *Sal* I and *Not* I, treated with Klenow, and re-ligated by T4 DNA ligase. Removal of two attP sites from pMG75-ATP4 was confirmed by PCR and sequencing using P18+P19 primers. Interestingly, during this process, 2 aptamer copies were lost (confirmed by PCR analysis and sequencing (P20+P21)). Therefore, this process resulted in a modified vector with 8 copies of aptamers, pMG75noP_ATP4_8apt. As the original vector, this vector contains a single copy of MYC tag and a single copy of HA tag. To increase tag affinity, we removed the single epitope tags from pMG75noP_ATP4_8apt and replaced it with a 3HA.

Next, we cloned two homologous regions (5'HR and3'HR) of PfmRPL13 into the modified vector, pMG75noP_ATP4_8apt_3HA. The 3'HR of PfmRPL13 (869 bp) was immediately downstream of the stop codon and was amplified via P22+P23 primers. It was cloned into the vector using *Sac* II and *Bst*E II sites. The 5'HR of PfmRPL13 was amplified via P24+P25 primers and cloned into the vector bearing 3'HR via *Bst*E II and *Sal* I sites. To avoid repetitive cutting by Cas9 in the transgenic parasites, the reverse primer (P25) of 5'HR included synonymous mutations within the pAIO-RL13-gRNA1 region. The pAIO-RL13-gRNA2 was located between the stop codon and 3'HR; therefore no synonymous mutations were needed. These procedures yielded the vector for double crossover recombination and knockdown studies, pMG75noP_PfmRPL13_8apt_3HA. The plasmid was linearized with *Eco*R V and transfected into parasites together with two gRNA constructs, pAIO-RL13-gRNA1 and pAIO-RL13-gRNA2.

4) For complementation studies in the knockdown parasites, we performed a second transfection by introducing an extra copy of yDHODH or PfmRPL13, respectively. Since the knockdown parasites already had bsd (blasticidin deaminase) from pMG75 (resistant to blasticidin) and yDHODH from pUF1 (resistant to DSM1), the hdhfr (human dihydrofolate reductase) marker (resistant to WR99210) was used for additional transfections. A copy of yDHODH was previously cloned into a pHH vector bearing an

hdhfr cassette (6). In case of PfmRPL13, we started with the pLN-PfmRPL13-3HA construct (described as above) by replacing the bsd marker with hdhfr and changing the 3HA tag to 3Myc. To do that, the pLN-PfmRPL13-3HA plasmid was digested with *Nco* I and *Bpu10* I to release the bsd marker. The hdhfr gene was amplified from pCC1 using primers (P26+P27) which had overlapping regions homologous to the pLN vector. The linearized pLN vector and the hdhfr fragment were annealed by InFusion cloning, resulting in a modified pLN vector with an hdhfr selectable marker, namely pLN-hdhfr-PfmRPL13-3HA. The PfmRPL13-3HA was then removed by digesting the vector with *Avr* II and *Afl* II. A synthetic DNA fragment of PfmRPL13 plus a 3Myc tag was synthesized as a gene block (Genewiz LLC), digested with *Avr* II and *Afl* II, and put into the vector by ligation, yielding the pLN-hdhfr-PfmRPL13-3Myc construct for complementation studies.

All primers and oligoes were purchased from Eurofins Genomics (Table S1). DNA fragments used for cloning were amplified with high fidelity DNA polymerases followed by sequencing confirmation (Genewiz LLC). All restriction endonucleases and DNA modifying enzymes were purchased from New England Biolabs®, Inc. All cloning steps involving pMG75-derived vectors were transformed into stable competent *E. coli* (New England Biolabs®, Inc) and bacteria were grown at 30 °C.

2. Parasite lines, parasite culture, and transfection.

P. falciparum strains used in this study included Dd2attB (2), NF54attB (7), D10 wildtype, and NF54 wildtype. Asexual *P. falciparum* parasites were cultured using RPMI medium supplemented with 0.5% Albumax II (Gibco by Life technologies) under a low oxygen atmosphere (6% O_2, 5% CO_2, 89% N_2), as described previously (8). Human blood (O^+) was purchased from the Interstate Blood Bank in Tennessee. Parasite transfections were performed in cultures with 5% rings using circular template plasmids (50 µg each electroporation) or linearized template plasmids (20-50 µg each electroporation) together with circular gRNA constructs (50 µg for each gRNA in each electroporation). Restriction endonucleases used

to linearize pL6-PfmRPL13-pKO and pMG75noP_ATP4_8apt were *Hinc* II and *Eco*R V, respectively. Drug selections were added 48 h post electroporation and maintained under the following concentrations: 5 nM WR99210 for hdhfr, 2.5 µg/ml blasticidin for blasticidin deaminase, 1.5 µM DSM1 for yDHODH (yeast dihydroorotate dehydrogenase), 125 µg/ml G418 for the neomycin selectable cassette, 2 µM 5-flurocytosine (5-FC) for FCU gene (yeast cytosine deaminase/uracil phosphoribosyl transferase).

3. Gene knockout approaches.

The CRISPR/Cas9 gene knockout approach was implemented (3) in two wildtype *P. falciparum* lines, D10 and NF54. They were individually transfected with a circular or linearized pL6-PfmRPL13-KO plasmid PfmRPL13 (containing two homologous regions and one gRNA) and pUF1-Cas9. These transfections were selected only with WR99210 for pL6-PfmRPL13-KO vector whereas Cas9 was expressed transiently. In parasite lines transfected with circular pL6-PfmRPL13-KO plasmid which still contains a negative selection marker, namely the FCU gene (the yeast cytosine deaminase and uracil phosphoribosyl transferase), we also performed negative selections with 5-FC in combination with WR99210 directly or after one round of drug off-and-on cycling. We also repeated transfections in D10 and NF54 lines using dual drug selections with WR99210 and DSM1. Since it has not been determined how long Cas9 is needed to obtain a knockout parasite in the literature, DSM1 was administered for one, two or four weeks post transfections along with WR99210.

4. Western blot.

Infected RBCs were treated with 0.05% saponin (MilliporeSigma) in PBS in the presence of 1x protease inhibitor cocktail (MilliporeSigma) and the parasitized pellet was resuspended in 2% SDS/62 mM Tris-HCl (pH 6.8) by repeated pipetting. The lysate was then spun down at 10,000 rpm for 5 min and the supernatant was then processed for SDS-PAGE analysis. Protein transfer, blocking, and other steps followed the standard protocol. The anti-HA primary antibody (sc-7392, Santa Cruz Biotechnology) was

used at 1: 10,000 and an HRP conjugated secondary anti-mouse antibody was used at 1: 10,000. The antibody against *P. falciparum* aldolase (ab38905, Abcam) was served as a positive control (1: 20,000).

5. Mitochondrion preparation (Mito-prep).

Mitochondrial isolation was performed according to a published protocol (9). For aTc plus parasites, cultures were tightly synchronized with alanine and expanded to 1.6-2.4 liters (4-6 T225 flasks). For aTc minus parasites, the culture was first grown under 250 nM aTc up to one T225 flask, and late stages were isolated by a Percoll gradient, as described above. The isolated parasites were washed 3 times with medium, and inoculated into new T225 flasks and maintained under regular RPMI (aTc minus) for 2 cycles or 4 cycles. After the desired growth, the parasites were harvested at trophozoite stages and lysed with 0.05% saponin in AIM buffer (120 mM KCl, 20 mM NaCl, 20 mM glucose, 6 mM HEPES, 6 mM MOPS, 1 mM MgCl2, 0.1 mM EGTA, pH 7.0) and washed three times with cold AIM buffer. The pellet was resuspended in argon deaerated MESH buffer (225 mM mannitol, 75 mM sucrose, 4.3 mM MgCl2, 0.25 mM EGTA, 10 mM HEPES [Tris], 5 mM HEPES [KOH], pH 7.4) containing 10 mM glucose and mitochondrial substrates (5 mM succinate and 5 mM L-malate) in the presence of 1 mM PMSF (Millipore Sigma) and 1 µl per ml fungal protease inhibitor cocktail (MilliporeSigma). The parasite suspension was added into a metal pressure chamber on ice and disrupted by N_2 cavitation, as previously described (9). The unbroken cells and cell debris were removed by centrifugation at 900 ×*g* for 6 min at 4 °C. The low speed supernatant was passed slowly (~0.2 ml/min) through a MACS CS column (Miltenyi Biotec) prewashed with MSEH buffer in a Vario MACS magnetic separation apparatus (Miltenyi Biotec) to remove most of the hemozoin from the preparation. This step was conducted at 4 °C. The eluted material was pelleted by centrifugation at 23,000 ×*g* for 20 min at 4 °C. The pellet was suspended in an appropriate volume (~500-1000 µl) of MSEH buffer containing 1.0 mM succinate, aliquoted in 50 µl aliquots, and used for enzymatic assays or stored at -80 °C.

6. ^{3}H-hypoxanthine growth inhibition assay.

Growth inhibition assays using ^{3}H-hypoxanthine incorporation were performed in 96 well plates as previously described (10). For drug assays, mixed stage parasites at 1% parasitemia and 3% hematocrit were exposed to compounds diluted by a serial dilution for 24 h. Then each well was pulsed with 10 µl of 0.5 µCi ^{3}H-hypoxanthine and incubated for another 24 h. Parasites were then lysed by freeze-thawing and nucleic acids were collected onto filters with a cell harvester (Perkin Elmer, MA). The filters were dried and counted with a Topcount scintillation counter (Perkin Elmer, MA) after addition of MicroScint O. For measuring parasite growth under aTc or in the absence of aTc for 1 cycle, parasites with 1% parasitemia and 3% hematocrit were inoculated into 96 well plates. ^{3}H-hypoxanthine was added 24 h later and incubated for another 24 h (in total of 48 h). For measuring growth for 2 cycles, parasites with 0.5% parasitemia and 3% hematocrit were inoculated. ^{3}H-hypoxanthine was added 72 h later and incubated for additional 24 h (in total of 96 h). Other steps followed the procedures described as above. GraphPad Prism 6 was used to graph the data.

7. Magnetic enrichment and transmission electron microscopy.

During knockdown experiments as described above, on day 6, the culture was spun down, re-suspended into 20% hematocrit, and bound to a MACS CS column prewashed with medium in the Vario MACS magnetic separation apparatus. Uninfected RBCs were washed from the CS column and the infected RBCs were harvested by washing the CS column after it was removed from the magnetic field. The enriched parasites, mostly late trophozoite/schizont stages, were washed with 100 mM sodium cacodylate and fixed with 2% paraformaldehyde/2.5% glutaraldehyde/100 mM sodium cacodylate at RT for 1 h. The fixed parasites were washed once with 100 mM sodium cacodylate and shipped to the Molecular Microbiology Imaging Facility at Washington University in St. Louis. Samples were then washed once with 100 mM sodium cacodylate and post-fixed in 1% osmium tetroxide (Polysciences Inc.) for 1 h. Samples were then rinsed extensively in dH_2O prior to en bloc staining with 1% aqueous uranyl acetate (Ted Pella Inc.) for 1 h. Following several rinses in dH_2O, samples were dehydrated in a graded series of ethanol and embedded in Eponate 12 resin (Ted Pella Inc.). Sections of 95 nm were cut with a

Leica Ultracut UCT ultramicrotome (Leica Microsystems Inc.), stained with uranyl acetate and lead citrate, and viewed on a JEOL 1200 EX Transmission Electron Microscope (JEOL USA Inc.) equipped with an AMT 8 megapixel digital camera and AMT Image Capture Engine V602 software (Advanced Microscopy Techniques).

Table S1. Sequences of primers and oligoes used in this study.

Primer ID	Description	Sequence
P1	RL13-F-BsiWI-AvrII	aTcgtacgcctaggATGATAAGAAGAAGCTTGATTAAATTAG
P2	RL13-R-BsiWI-AflII	GTcgtacgcttaagCAAAATGGTAAAGGTCTTTATATC
P3	RL13-5fF-SacII	ttCCGCGGCAAAAAAGGTCCCGGAGTACA
P4	RL13-5fR-AflII	aaCTTAAGTTGAAAAAGGGTTAATGTGCTG
P5	RL13-3fF-EcoRI	aaGAATTCGTTGATATTTTTTCAGAAGAAC
P6	RL13-3fR-NcoI	aaCCATGGTTTATGTGCTGTGTTATGTTG
P7	RL13-oligo1	CATATTAAGTATATAATATTGGCATATTCTTCTTTAAAAAGTTTTAGAGCTAGAAATAGC
P8	RL13-oligo2	GCTATTTCTAGCTCTAAAACTTTTTAAAGAAGAATATGCCAATATTATATACTTAATATG
P9	RL13KO_gRNA N20	GGCATATTCTTCTTTAAAAA
P10	N20CheckR	ATATGAATTACAAATATTGCATAAAGA
P11	gRNArevo	TAGGAAATAATAAAAaagcacc
P12	RL13-oligo5	CATATTAAGTATATAATATTGATATTGTTACAAAATGGTAAGTTTTAGAGCTAGAAATAGC
P13	RL13-oligo6	GCTATTTCTAGCTCTAAAACTTACCATTTTGTAACAATATCAATATTATATACTTAATATG
P14	RL13apt_gRNA1 N20	ATATTGTTACAAAATGGTAA

P15	RL13-oligo7	CATATTAAGTATATAATATTGTAACACAGCACATAAACATTGTTTTAGAGCTAGAAATAGC
P16	RL13-oligo8	GCTATTTCTAGCTCTAAAACAATGTTTATGTGCTGTGTTACAATATTATATACTTAATATG
P17	RL13apt_gRNA2 N20	TAACACAGCACATAAACATT
P18	revattPF	GTTAATTCATCAAATAGCATGCCTG
P19	revattPR	AGCTGGCACGACAGGTTTCC
P20	pMG75AptF	CACCAGGTGATTATAAAGATGATGATG
P21	pMG75AptR	GTAGACCCCATTGTGAGTAC
P22	RL13_3UTRF	aTcCGCGGtCTTAAGCATTAGTCCACTTTTTTAATATAACATATTATGCAC
P23	RL13_3UTRR	ctGGTTACCaTcATTTTGATATGTACTTTATACTTGGC
P24	RL13_5HRF	ctGGTTACCtaGATATCaaCCGCGGataTcAGCACATTAACCCTTTTTC
P25	RL13_5HRR	ATGTCGACCTGCAGTAATATTGTGAATGTCTTTATATCTTGCTGCTCTTCC
P26	hdhfrFToBSD	GCTTATATATATACACACACCTAAAACTTACAAACCGGTccatggaaaaATGCATGGTTCGCTAAACTGCATC
P27	hdhfrRToBSD	AATCTATTATTAAATAAATTTAATGGGGTACCTTAGCTCCGGAtTAATCATTCTTCTCATATACTTCAAATTTGTAC

Figure S1A

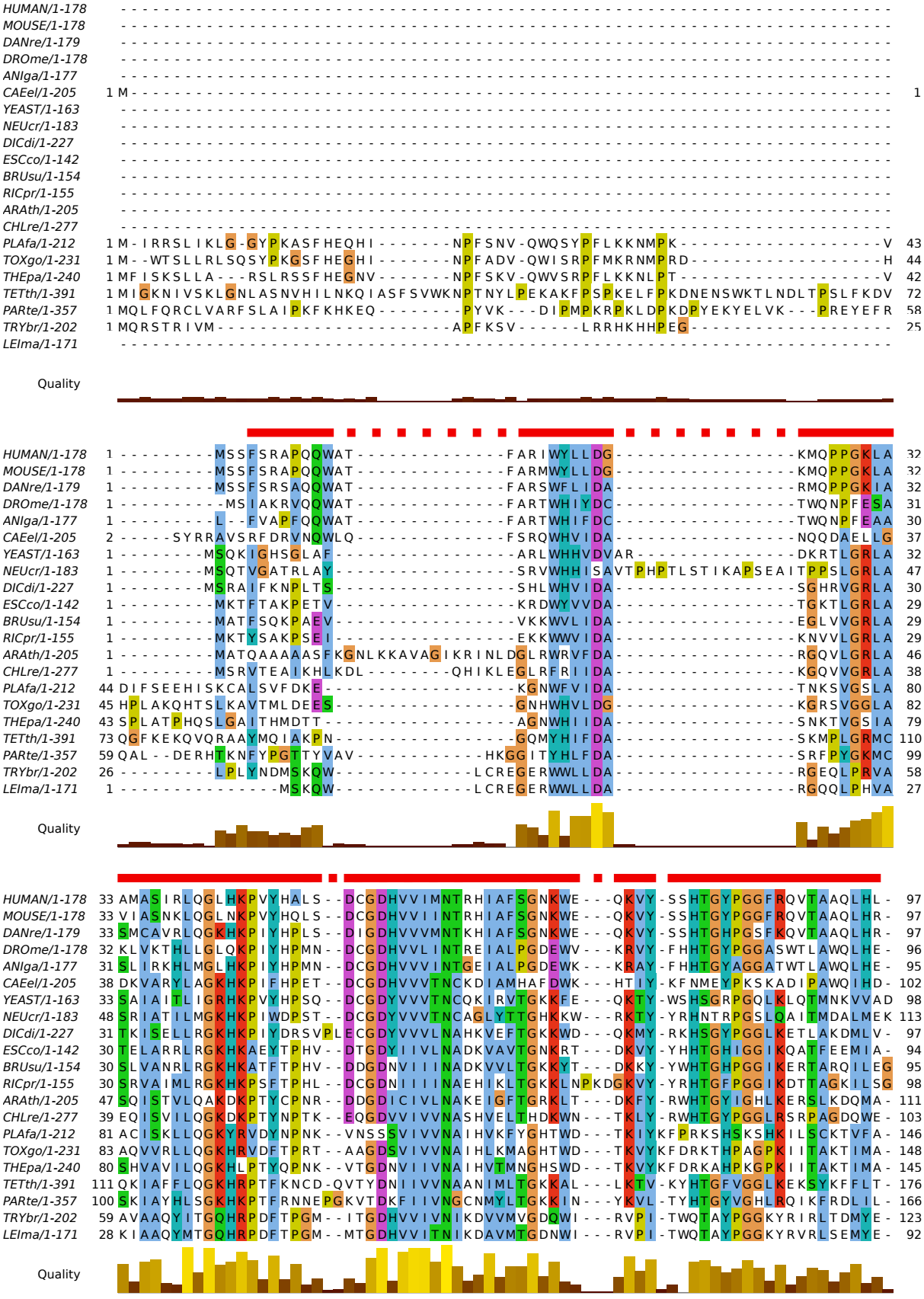
HUMAN/1-178
MOUSE/1-178
DANre/1-179
DROme/1-178
ANIga/1-177
CAEel/1-205
YEAST/1-163
NEUcr/1-183
DICdi/1-227
ESCco/1-142
BRUsu/1-154
RICpr/1-155
ARAth/1-205
CHLre/1-277
PLAfa/1-212
TOXgo/1-231
THEpa/1-240
TETth/1-391
PARte/1-357
TRYbr/1-202
LEIma/1-171
Quality

Figure S1A continuation

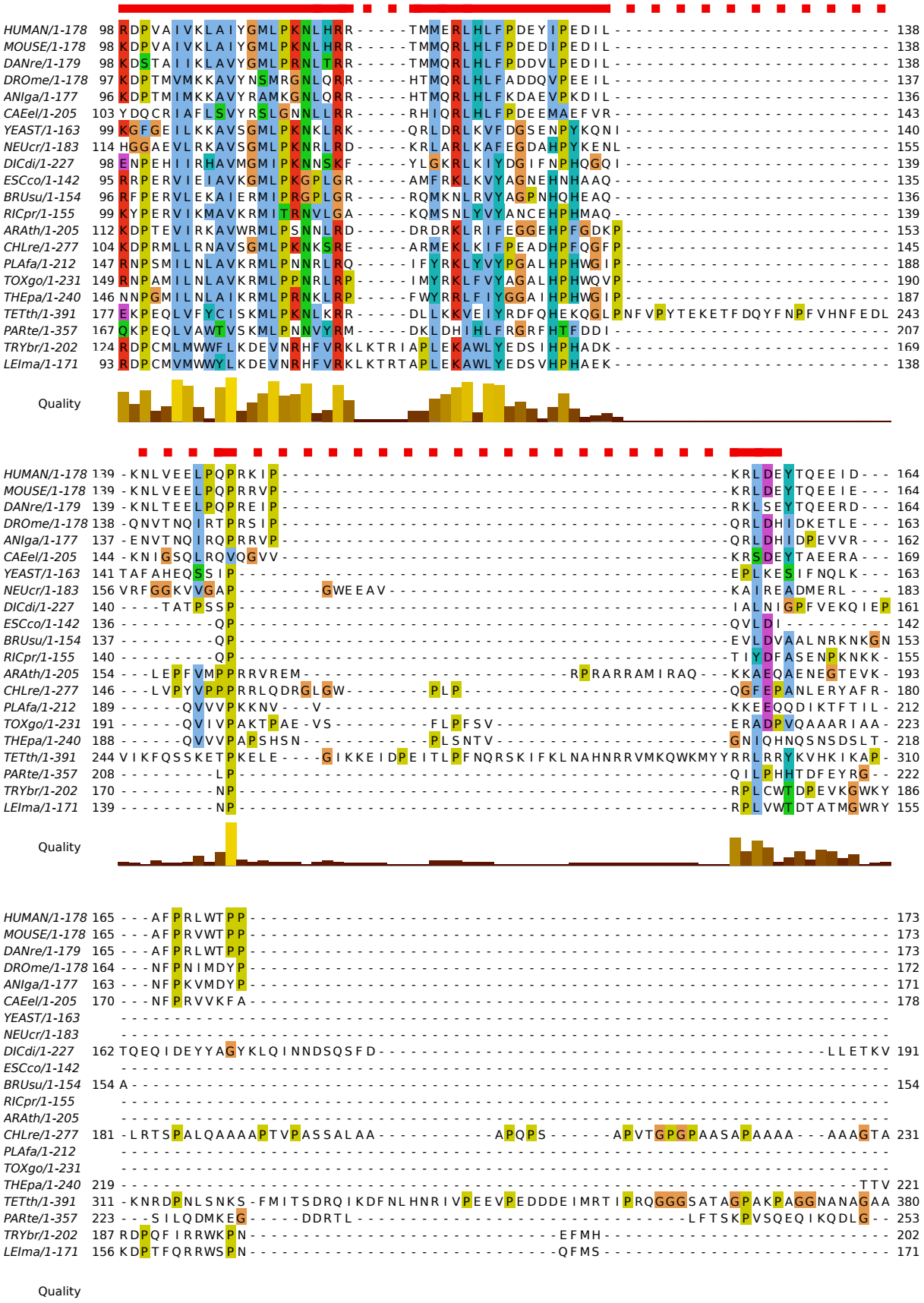

Figure S1A continuation

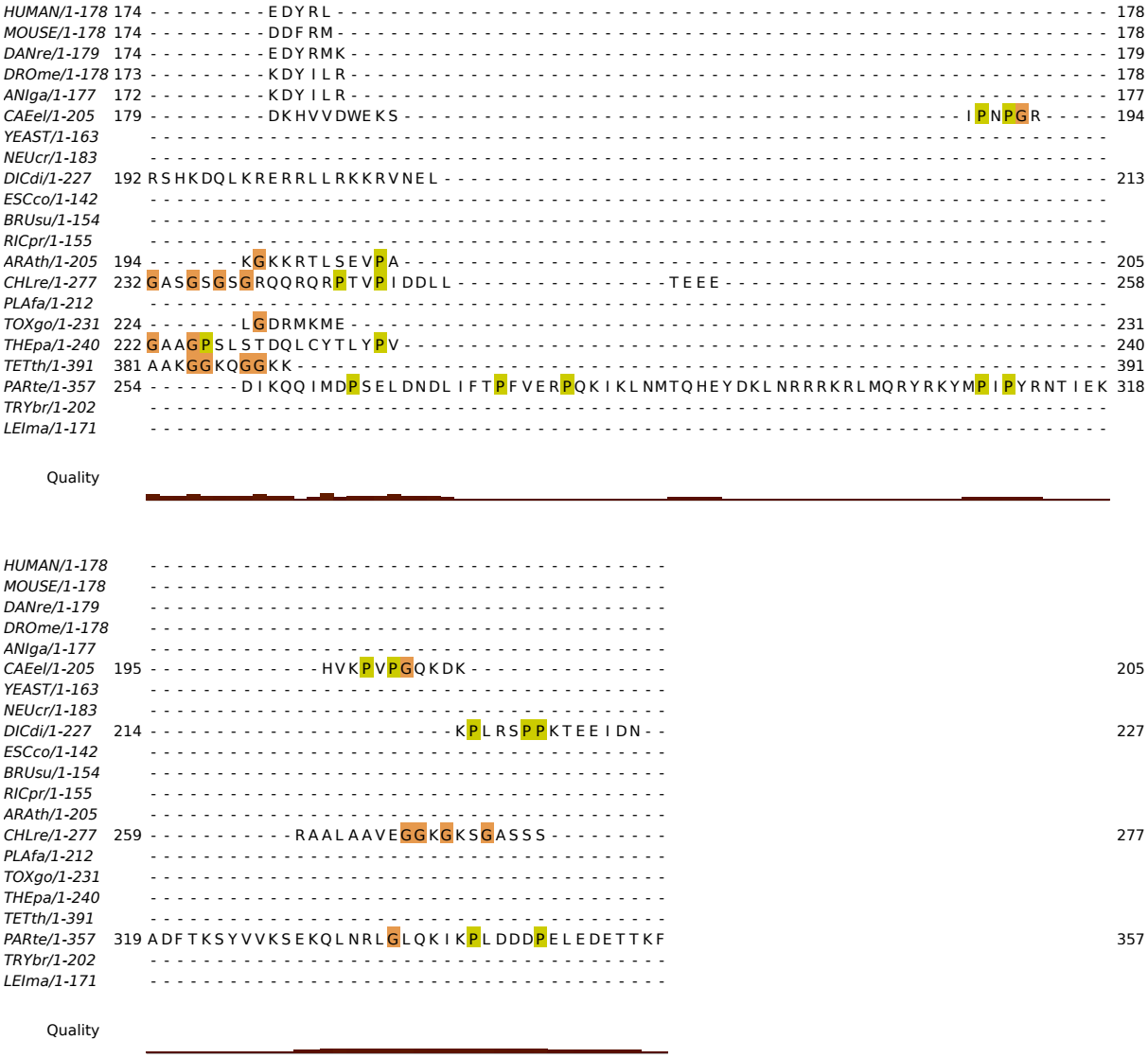

Figure S1B

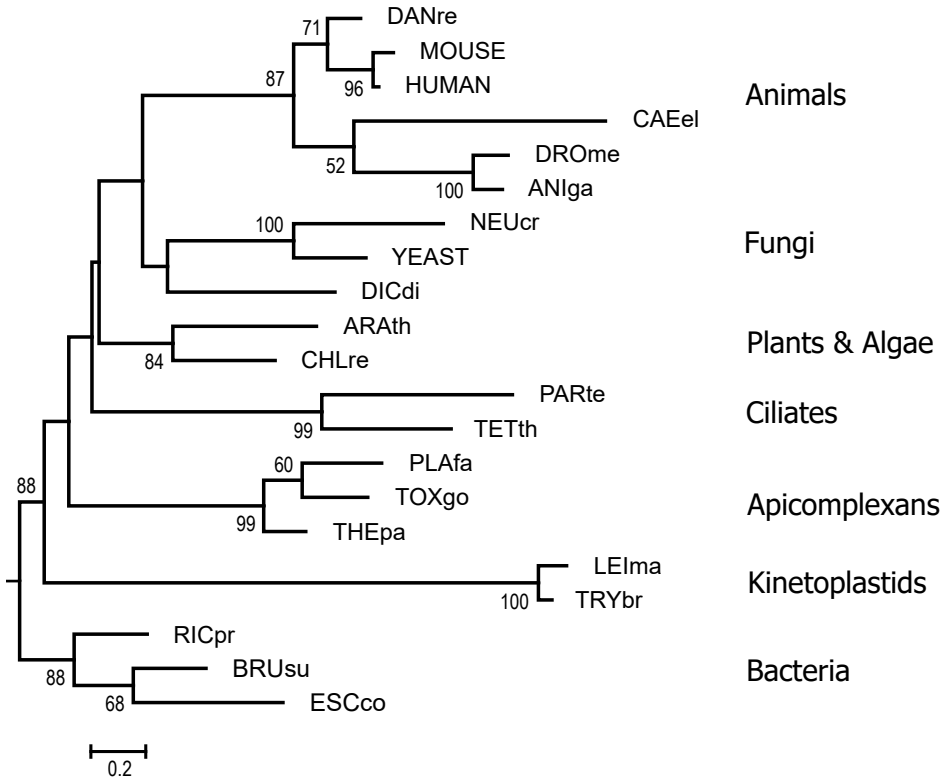

Figure S1. (A) Multiple sequence alignment of a representative set of mitochondrial RPL13 proteins from a broad range of phyla and sample proteobacterial RPL13 proteins ("outgroup"). The proteins chosen mirror those used in a previous study of mitoribosomal proteins (11), with the addition of three alveolate proteins (*Toxoplasma gondii*, *Theileria parva*, *Paramecium tetraurelia*) and one vertebrate (*Danio rerio*) and removal of the vertebrate *Tetraodon nigroviridis*. Sequence alignment was performed with the MAFFT server using L-INS-i method and homologues addition (12). The alignment was formatted for display with JALVIEW using the Clustal color scheme, which reflects the chemical property of conserved amino acids at each alignment position (13). The solid red bars indicate the columns of the alignment that match the Interpro family model "Ribosomal Protein L13, bacterial-type" (IPR005823) (which model includes mitochondrial and chloroplast L13 subunits). Specific IDs of the protein sequences aligned (UniProt designations): HUMAN (*Homo sapiens*)Q9BYD1, MOUSE (*Mus musculus*) Q9D1P0, *Danio rerio*Q504D1, *Drosophila melanogaster*Q9VJ38, *Anopheles gambiae* Q7Q191, *Caenorhabditis elegans*Q95QL2, YEAST (*Saccharomyces cerevisiae*) Q12487, *Neurospora crassa*Q7SBV6, *Dictyostelium discoideum*Q554U7, *Arabidopsis thaliana*Q7XA68, *Chlamydomonas reinhardtii*A8J810, *P. falciparum*O96222, *T. gondii* A0A125YJY5, *T. parva*Q4N8U5, *Tetrahymena thermophila*W7X626, *P. tetraurelia*A0C5X1, *Trypanosoma brucei* Q580D5, *Leishmania major* Q4Q2H6, *Escherichia coli* P0AA10, *Brucella suis*Q8G1C8, and *Rickettsia prowazekii*Q9ZDU1.

(B) Phylogenetic tree inferred for the set of diverse mitochondrial RPL13 and proteobacterial RPL13 sequences. Apicomplexan mRPL13 subunits form a well-supported, separate clade within the mitochondrial grouping (the latter defined by setting the root with the proteobacterial clade). The tree was inferred by maximum likelihood analysis (PhyML(14)). Bootstrap support is shown for nodes with greater than 50% support.

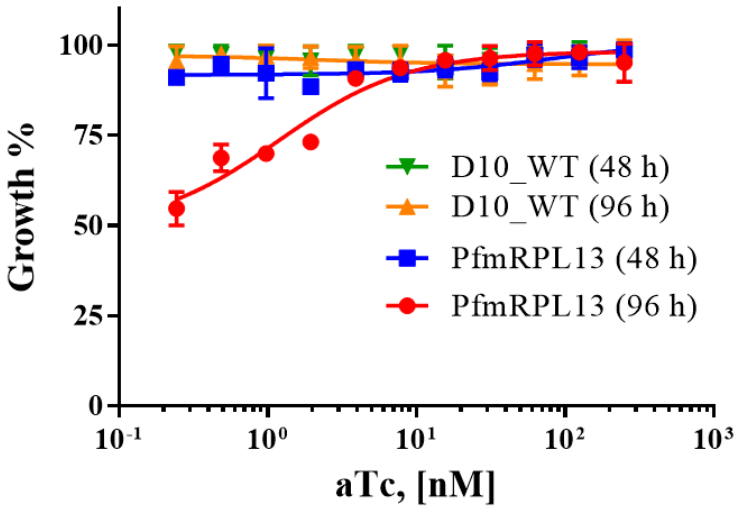

Figure S2. Growth of PfmRPL13 knockdown parasites with various concentrations of aTc for one and two cycles using ^{3}H-hypoxanthine incorporation. aTc was diluted from 250 nM in a serial dilution with a factor of 2. The lowest concentration was 0.24 nM. D10 wildtype served as a control. Error bars were derived from n=3 biological replicates.

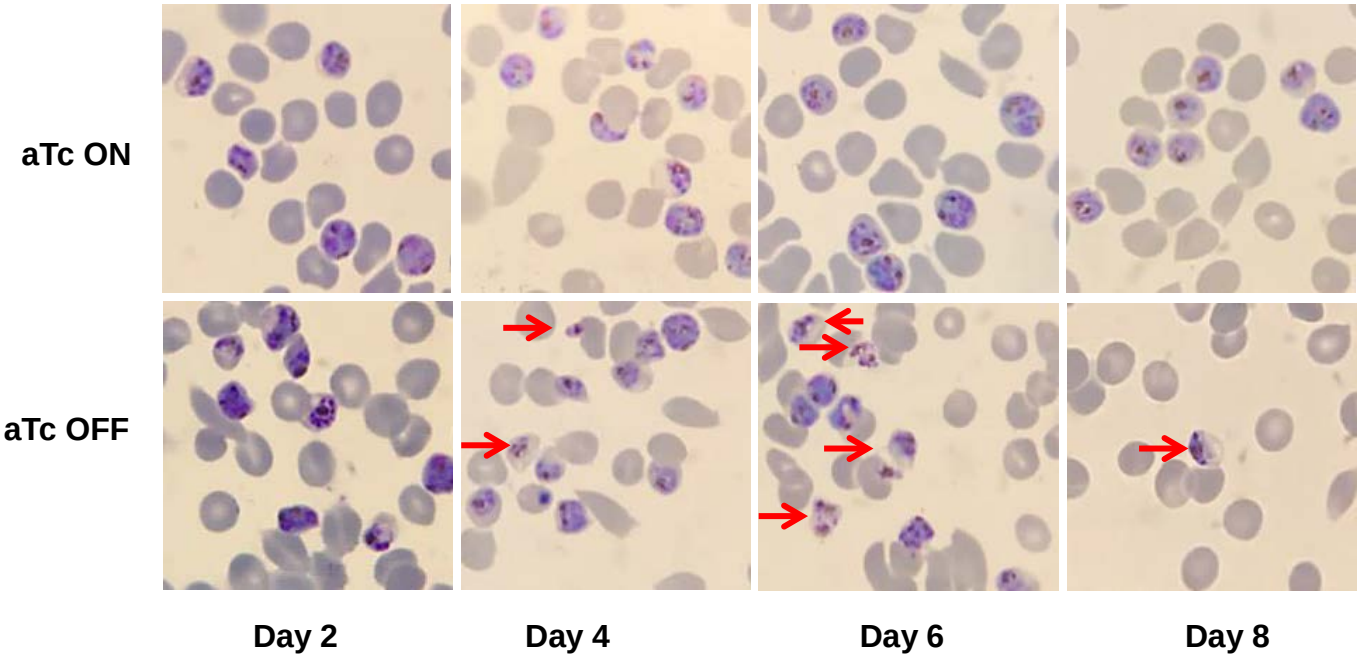

Figure S3. Morphological changes of PfmRPL13 knockdown parasites on Giemsa stained thin blood smears. Red arrows indicate dead or morphologically deteriorating parasites after aTc was removed from the culture. To display multiple parasites in one field under the microscope, late stage parasites of the cultures with or without aTc were enriched by a Percoll gradient.

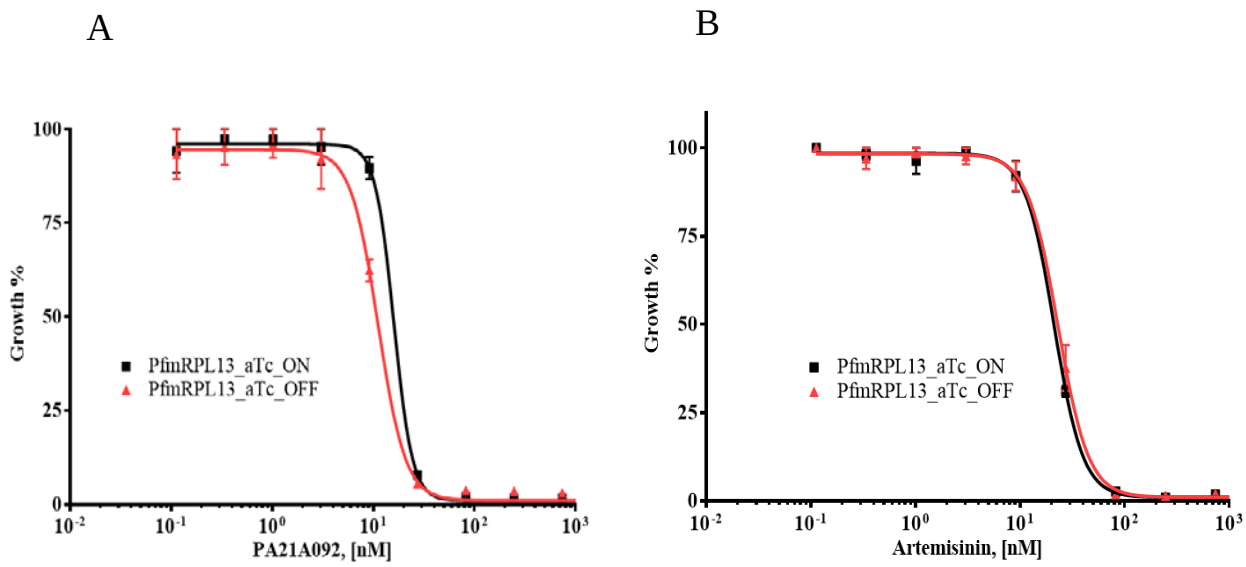

Figure S4. PfmRPL13 knockdown parasites show equal sensitivity to PA21A092 and artemisinin in the presence or absence of aTc. Growth inhibition assays were carried out using ^{3}H-hypoxanthine incorporation in 48 h. PfmRPL13 knockdown parasites were grown in the absence of aTc for 3 cycles before exposed to PA21A092 (15) or artemisinin. EC50s of PA21A092 in the presence or absence of aTc are 15.9 nM and 11.2 nM, respectively. EC50s of artemisinin in the presence or absence of aTc are 21.2 nM and 23.1 nM, respectively.

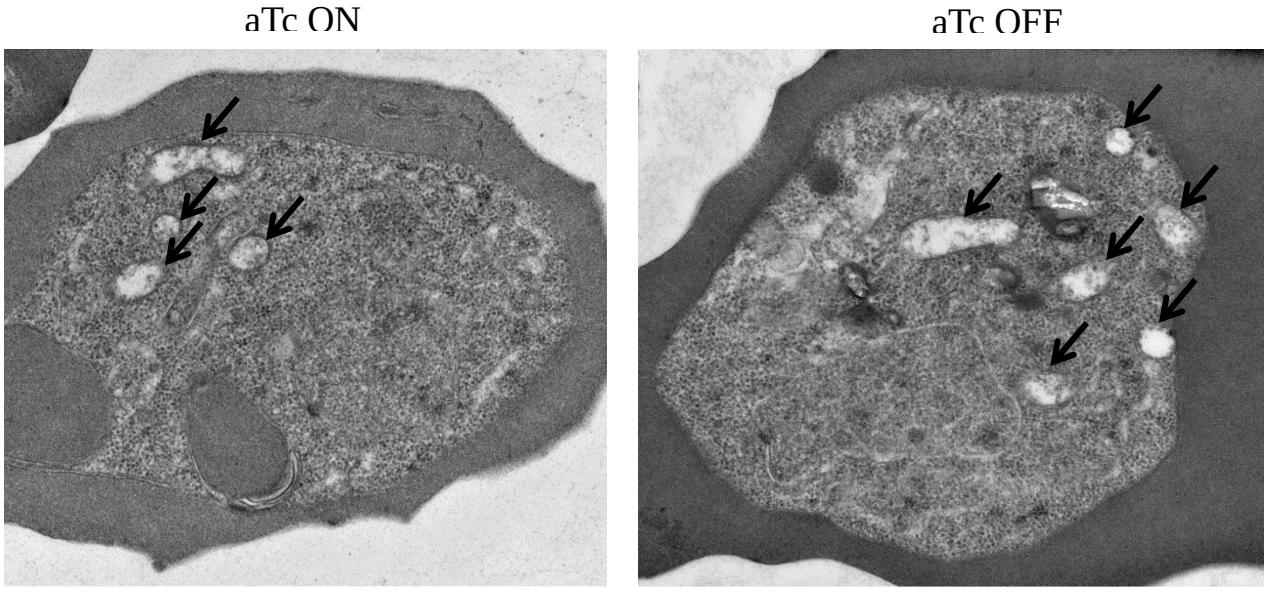

Figure S5. Mitochondrial morphologies of D10 wildtype parasites maintained with or without aTc and examined by transmission electron microscopy (TEM) studies. Black arrows on TEM images indicate cross sections of the parasite mitochondria.

References

1. Balabaskaran Nina P, Morrisey JM, Ganesan SM, Ke H, Pershing AM, Mather MW, Vaidya AB. 2011. ATP synthase complex of Plasmodium falciparum: dimeric assembly in mitochondrial membranes and resistance to genetic disruption. J Biol Chem 286:41312-22.
2. Nkrumah LJ, Muhle RA, Moura PA, Ghosh P, Hatfull GF, Jacobs WR, Jr., Fidock DA. 2006. Efficient site-specific integration in Plasmodium falciparum chromosomes mediated by mycobacteriophage Bxb1 integrase. Nat Methods 3:615-21.
3. Ghorbal M, Gorman M, Macpherson CR, Martins RM, Scherf A, Lopez-Rubio JJ. 2014. Genome editing in the human malaria parasite Plasmodium falciparum using the CRISPR-Cas9 system. Nat Biotechnol 32:819-21.
4. Ganesan SM, Falla A, Goldfless SJ, Nasamu AS, Niles JC. 2016. Synthetic RNA-protein modules integrated with native translation mechanisms to control gene expression in malaria parasites. Nat Commun 7:10727.
5. Spillman NJ, Beck JR, Ganesan SM, Niles JC, Goldberg DE. 2017. The chaperonin TRiC forms an oligomeric complex in the malaria parasite cytosol. Cell Microbiol 19.
6. Painter HJ, Morrisey JM, Mather MW, Vaidya AB. 2007. Specific role of mitochondrial electron transport in blood-stage Plasmodium falciparum. Nature 446:88-91.
7. Adjalley SH, Johnston GL, Li T, Eastman RT, Ekland EH, Eappen AG, Richman A, Sim BK, Lee MC, Hoffman SL, Fidock DA. 2011. Quantitative assessment of Plasmodium falciparum sexual development reveals potent transmission-blocking activity by methylene blue. Proc Natl Acad Sci U S A 108:E1214-23.
8. Ke H, Lewis IA, Morrisey JM, McLean KJ, Ganesan SM, Painter HJ, Mather MW, Jacobs-Lorena M, Llinas M, Vaidya AB. 2015. Genetic investigation of tricarboxylic acid metabolism during the Plasmodium falciparum life cycle. Cell Rep 11:164-74.
9. Mather MW, Morrisey JM, Vaidya AB. 2010. Hemozoin-free Plasmodium falciparum mitochondria for physiological and drug susceptibility studies. Mol Biochem Parasitol 174:150-3.
10. Ke H, Morrisey JM, Ganesan SM, Painter HJ, Mather MW, Vaidya AB. 2011. Variation among Plasmodium falciparum strains in their reliance on mitochondrial electron transport chain function. Eukaryot Cell 10:1053-61.
11. Smits P, Smeitink JA, van den Heuvel LP, Huynen MA, Ettema TJ. 2007. Reconstructing the evolution of the mitochondrial ribosomal proteome. Nucleic Acids Res 35:4686-703.
12. Katoh K, Rozewicki J, Yamada KD. 2017. MAFFT online service: multiple sequence alignment, interactive sequence choice and visualization. Brief Bioinform doi:10.1093/bib/bbx108.
13. Waterhouse AM, Procter JB, Martin DM, Clamp M, Barton GJ. 2009. Jalview Version 2--a multiple sequence alignment editor and analysis workbench. Bioinformatics 25:1189-91.
14. Guindon S, Dufayard JF, Lefort V, Anisimova M, Hordijk W, Gascuel O. 2010. New algorithms and methods to estimate maximum-likelihood phylogenies: assessing the performance of PhyML 3.0. Syst Biol 59:307-21.
15. Das S, Bhatanagar S, Morrisey JM, Daly TM, Burns JM, Jr., Coppens I, Vaidya AB. 2016. Na+ Influx Induced by New Antimalarials Causes Rapid Alterations in the Cholesterol Content and Morphology of Plasmodium falciparum. PLoS Pathog 12:e1005647.